magnetochemistry

MDPI

Article

Effect of Magnetic Coupling on the Optical Properties of Oxide Co Nanowires on Vicinal Pt Surfaces

Kseniya M. Tsysar [1,*], Dmitry I. Bazhanov [1,2] and Ekaterina M. Smelova [1]

[1] Faculty of Physics, M.V. Lomonosov Moscow State University, GSP-1, 1-2 Leninskiye Gory, 119991 Moscow, Russia
[2] Federal Research Center "Computer Science and Control", Russian Academy of Sciences (FRC CSC RAS), Vavilova St. 44/2, 119333 Moscow, Russia
* Correspondence: smelova_k_m@physics.msu.ru

Abstract: Nowadays, modern scientific research has sparked a renewed interest to study the interaction of electromagnetic field (EM) with magnetic nanostructures and in particular in nanophotonics and spintronics. The current work is devoted to an ab initio study of the magneto-optical properties of step-decorated oxide Co nanowires (1D oxides) on vicinal Pt surfaces. Theoretical calculations of the magnetic moments are based on ab initio spin-polarized density-functional theory (DFT) including a self-consistent treatment of spin-orbit coupling. The first-principles calculations revealed the effect of magnetic coupling between cobalt spins on refractivity and extinction spectra of these 1D oxides governed by atomic structure and cobalt-oxygen interaction within a nanowire at the step edge. The emergence of a sharp pronounced peak in the spectral difference of the refractive indexes has been observed between ferromagnetic and antiferromagnetic configurations of the nanowire. Anisotropy of an extinction coefficient in the terahertz (THz) range of the spectra was established for oxide Co nanowires in an antiferromagnetic state in contrast with a ferromagnetic one.

Keywords: density functional theory; Co oxide nanowires; magneto-optics; refractivity; dielectric constant; Pt vicinal surface; nanomagnetism

Citation: Tsysar, K.M.; Bazhanov, D.I.; Smelova, E.M. Effect of Magnetic Coupling on the Optical Properties of Oxide Co Nanowires on Vicinal Pt Surfaces. *Magnetochemistry* **2023**, *9*, 72. https://doi.org/10.3390/magnetochemistry9030072

Academic Editors: Derang Cao and Roman Adam

Received: 16 January 2023
Revised: 23 February 2023
Accepted: 27 February 2023
Published: 2 March 2023

1. Introduction

In recent years, the study of the interaction of an electromagnetic (EM) field with low-dimensional structures with the possibility of further application in magnetic recording technology, spintronics and magnonics is of particular scientific interest [1–4]. The development of this field of science was affected by the appearance of modern lasers, which can generate ultra-short pulses in the terahertz frequency range, which corresponds to the frequency of ferromagnetic transitions and makes it possible to study ultrafast magnetism [2]. Furthermore, the time-dependent properties of light waves can cause transient effects of spin polarization in oxides [2] and metals [3,4]. The most sought-after destination direction in this research area is the study of the interaction of EM field with magnetic metal nanostructures [5]. Ortega et al. first found experimentally the interplay between magnetic and optical properties of special magnetic Ag/FeCo metallic core/shell nanoparticles [5]. They revealed the dependence of optical characteristics of reflected light on the magnetic configuration of these special particles. This study demonstrated that low-dimensional structures with several magnetic configurations are perspective systems for the study of magneto-optical properties. Therefore, one of the most attractive research studies in this area is the study of the magneto-optical properties of one-dimensional (1D) magnetic nanowires, as shown in the work of Belotelov et al. [1]. Gambardella et al. first found experimentally the emergence of long magnetic order in Co nanowires on vicinal Pt(997) surface [6]. Further extensive experimental and theoretical studies showed that various 3d−5d monatomic NWs with desirable magnetic properties (large magnetic moments, giant exchange and MAE) can be grown at low temperatures in a self-organized manner at

the step edges of vicinal surfaces [7–12]. Our own studies revealed the existence of several magnetic configurations in systems of freestanding and supported metal nanowires on a nonmagnetic metal substrate [13–15]. All these studies demonstrate that one-dimensional nanowires can be applied in various areas of technology, including devices for recording and storing information. However, a few major obstacles prevent their further technological applications, for example, the presence of gas impurities (such as O, H, N, C, etc.) during the epitaxial growth of NWs [16–19]. These impurities can incorporate directly into the nanowire, changing its interatomic interactions [20]. This can strongly impact the magnetic properties of NWs, such as local magnetic moment, exchange coupling and magnetic anisotropy [19–24]. However, the embedding of impurities into nanowires can also lead to the emergence of new physical properties. The recent experiments revealed that the presence of oxygen at step edges decorated by metal magnetic NWs can lead to the formation of novel low-dimensional magnetic oxides [25–27]. The formation of quasi-1D CoO nanostripes was observed experimentally on a vicinal Pd(1,1,23) surface [28]. The step decoration of a vicinal Rh(553) surface with monatomic rows of Ni adatoms followed by selective oxidation admitted to generating the pseudomorphically strained 1D oxides with perfect NiO and NiO_2 stoichiometries [29]. Moreover, oxides of bimetallic Ni-Rh NWs were obtained by an exclusive oxidation of self-assembled Ni nanostripes grown on a stepped Rh(111) surface with increasing oxygen coverage [30]. Therefore, the usage of different vicinal metal surfaces as a natural template for the formation of novel metal oxide nanostructures via a step decoration is a suitable strategy to fabricate new metal 1D oxides for advanced magnetics studies in low dimensions. Our recent study has shown that these 1D oxide NWs can possess magnetic properties [31,32]. Moreover, the presence of oxygen impurities can lead to more efficient absorption of EM radiation due to the change in the electronic state of the O atom [33]. Furthermore, it was shown that the impact of EM radiation on low-dimensional structures leads to a change in the electronic structure and spin state. Therefore, the further extended theoretical and experimental studies of the interplay between magnetic and optical properties of one-dimensional oxide NWs are very important from fundamental and practical points of view. To keep controlling or manipulating the magnetic properties of these low-dimensional structures under an EM field can be considered a very promising task.

In the present work, we have carried out an ab initio study of the effect of magnetic coupling on the optical properties of one-dimensional oxide Co NWs on vicinal Pt(332) and Pt(322) surfaces, since such surfaces can be employed as a perfect template for growing the one-dimensional cobalt nanostructures at the step edges, as it was shown experimentally by Gambardella [6]. The oxygen adsorption sites were chosen according to Bandlow et al., work [34]. The Pt(332) and Pt(355) surfaces have the same local atomic structure at the step edges, but different lengths of the open neighboring terraces between steps, which does not play a significant role in the effects at the step edge on the magneto-optical properties of oxide Co nanowires. The first-principles calculations revealed the effect of magnetic coupling between Co atoms on refractivity and extinction spectra of 1D oxide nanowires at the step edge. We demonstrate that the anisotropy of an extinction coefficient in the terahertz (THz) range of the spectra was established for oxide Co nanowires in an antiferromagnetic (AFM) state in contrast with the ferromagnetic (FM) one. The novelty of our work is in the comprehensive study of the magneto-optical properties of one-dimensional cobalt oxide nanowires and in the study of the effect of magnetic coupling in the nanowire on its spectral characteristics, which is necessary for the further possibility of using EM radiation to recognize the magnetic state of the system under study.

2. Methods

The study of the magneto-optical properties of the oxide Co NWs was carried out using the program Vienna Ab-initio Simulation Package (VASP.5.2) (VASP Software GmbH, Sensengasse 8/12 A-1090, Vienna, Austria) code which is based on the density functional theory (DFT) [35]. Spin-polarized calculations within the framework of density-functional

theory (DFT) are a powerful tool to describe the magnetism of *d*-electrons in transition metals. Such calculations are the basis for a quantitative theoretical determination of spin magnetic configurations of studied systems and also for the explanation of the basic mechanisms, which lead to the occurrence of magnetism in these systems [12–15,23]. The calculations presented in this paper were based on the self-consistent Kohn–Sham equations [36]. Electronic states were described using the basis of plane waves. The cutoff energy for plane wave basis of 400 eV was used. The increase in the cutoff energy of more than 400 eV does not enhance of the accuracy of calculations. The calculations were performed using the Local Density Approximation (LDA) for exchange-correlation functional with the GW approach and PAW (Projector Augmented-Wave) pseudopotentials [36,37]. The integration over Brillouin Zone (BZ) was performed using the tetrahedron method with Blöchl corrections. To calculate the total energy of the system we carried out the integration in reciprocal space with a special *k*-points mesh of $10 \times 10 \times 1$ constructed according to the Monkhorst-Pack scheme [38,39]. The structure of oxide NWs has been represented by means of three-dimensional supercell with periodic boundary conditions. The Pt substrate was constructed by means of a 5 atomic layer slab with a vacuum region (~10 Å) in order to avoid spurious interactions between them in supercell (Figure 1). Recent experimental studies of Bandlow [34], Klikovitz [40], and others have shown that oxidation proceeds along the step edge (*y*-axis in supercell) of the surface. Oxide Co NW was represented by an atomic chain aligned along the step edge of the vicinal Pt surface. Co atoms in oxide NW were placed in highly symmetric positions close to the platinum step edge, while the oxygen atoms were placed in accordance with the previous experimental and theoretical studies [40]. Two types of step edge oxidation were studied: low oxidized state, corresponding to the step edge oxidation in case of 0.1 monolayer (ML) coverage of Pt(111) surface (CoO configuration); and high oxidized state with oxygen coverage of 0.4 ML (CoO_2 configuration). Since the metal oxide nanowires are systems with strong electronic interaction, the DFT + U approach should be considered to give more accurate results. In our work, the correlation effects in localized *d*-electrons of cobalt atoms in oxide Co nanowire were treated with the LSDA + *U* approach, where *U* is an effective interaction parameter $U_{eff} = U - J$ of Dudarev et al. [41]. Recent experimental and theoretical studies have shown that $U_{eff} = 3.3$ eV describes satisfactorily the crystal structure and electronic properties of bulk CoO oxide [42], while the value of $U_{eff} = 1.0$ eV resulted in the best agreement with the experiment of the calculated geometric and electronic structures of the low-dimensional ultrathin CoO nanofilms [43]. Herein, the step-decorated oxidized Co nanowires can be considered as a prototype of low-dimensional oxide nanostructures. Therefore, in all calculations of the present work, we have used the value of $U_{eff} = U - J = 1.0$ eV with the screened exchange parameter *J* as 0.92 eV, which better describes the low-dimensional systems.

A structural relaxation was performed via a quasi-Newton algorithm, using the exact Hellmann–Feynman forces acting on each atom [35]. The total energies of the system were converged up to 1 meV/atom, while the residual force acting on each atom was less, than 0.01 eV/Å. After the study of magnetic properties, we studied the optical properties of oxide Co NWs such as refractivity, extinction and reflectivity characteristics. For this, the real and imaginary parts of the dielectric function were calculated following the formulation proposed by Gajdos et al., using the VASP code and the LOPTICS method [35,44,45]. The imaginary part of the dielectric function is taken to as a weighted sum of direct transitions from the occupied valence band states to unoccupied conduction band states (see Equation (1)), and the real part is determined from the Kramers–Kronig transformation (see Equation (2)) [44].

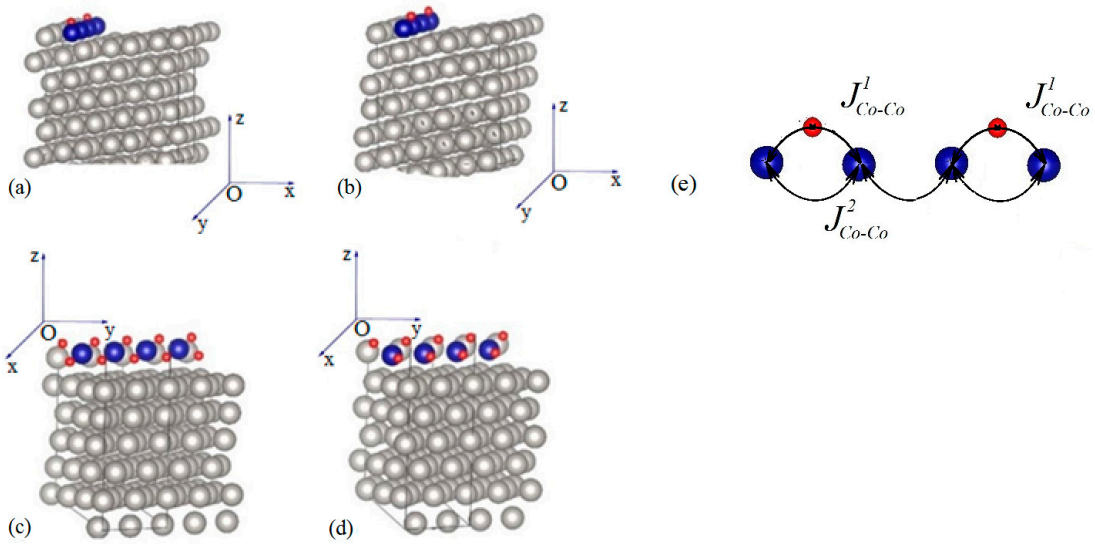

Figure 1. Model of studied metal oxide nanowire: low oxidized state CoO nanowire Pt(332) (**a**) and Pt(322) (**b**); and high oxidized state CoO_2 nanowire Pt(332) (**c**) and Pt(322) (**d**); Pt—grey spheres, Co—blue spheres, O—red spheres; (**e**) exchange channels between Co atoms: indirect exchange channel J^1_{Co-Co} through oxygen atoms, direct exchange channels between Co atoms J^2_{Co-Co}.

$$\varepsilon_2^{\alpha\beta}(\omega) = \frac{4\Pi^2 e^2}{\Omega} \lim_{q\to\infty} \sum_{c,v,k} 2\omega_k \delta(\epsilon_{ck} - \epsilon_{vk} - \omega) \times \langle u_{ck+e_\alpha q} | u_{vk} \rangle \langle u_{ck+e_\alpha q} | u_{vk} \rangle^* \quad (1)$$

$$\varepsilon_1^{\alpha\beta}(\omega) = 1 + \frac{2}{\Pi} \mathrm{P} \int_0^\infty \frac{\varepsilon_2^{\alpha\beta}(\omega')\omega'}{\omega'^2 - \omega^2 + in} d\omega' \quad (2)$$

The Drude-like term, with the anisotropic intraband plasma frequency tensor, was included in the dielectric function. The dielectric response for electric field normal to the interface (*z*-direction) differs from that of the in-plane directions (*x*-, *y*-directions). Since in our model we have considered the normal light incidence so the photon itself is propagating in the *z*-direction that means for both linearly or circularly polarized light the electric field will be in the *xy*-plane. For all optical calculations, we must have enhanced the total number of bands to achieve good convergence of calculations of the dielectric tensor. A more dense *k*-point mesh is also required to effectively sample the Brillouin zone and accurately determine the optical properties of a system in comparison to calculations of magnetic properties and electronic structure of oxide nanowires. Therefore, for all optical calculations, we used a dense $10 \times 10 \times 1$ *k*-point mesh. Our test calculations have shown that more dense mesh has no effect on the accuracy of dielectric function calculations. An energy cutoff of 500 eV was found to be sufficient for optical calculations as well, and no noticeable change in the dielectric function when cutoff energy was increased up to 700 eV. The real and imaginary components of the complex refractive index (n and κ) can be calculated directly from the real (ε_1) and imaginary (ε_2) parts of the dielectric function (see Equation (3)).

$$n = \left[\frac{\sqrt{\varepsilon_1^2 + \varepsilon_2^2} + \varepsilon_1}{2} \right]^{\frac{1}{2}}, \kappa = \left[\frac{\sqrt{\varepsilon_1^2 + \varepsilon_2^2} - \varepsilon_1}{2} \right]^{\frac{1}{2}} \quad (3)$$

Here, κ is the extinction coefficient or the imaginary component of the complex refractive index.

3. Results and Discussion

We perform an ab initio study of magneto-optical properties of 1D oxide Co nanowires, as a prototype of a 1D metal-oxide system, placed at the step edges of a vicinal Pt(111) surface. Two kinds of step edges on vicinal Pt(111) surface with {100}- and {111}-type facets have been considered since the oxidation process is found to be step-oriented [34,40]. For this purpose, two types of vicinal platinum (111) surface (corresponding to Pt(322) and Pt(332) surfaces, respectively) were considered where the oxidation of step edges was investigated. Figure 1 shows the all models of oxide Co NWs studied in the present work: the CoO nanowire, with one oxygen atom per two Co atoms in NW, corresponding to a low-oxidized state (Figure 1a,b); and dioxide CoO_2 NW with four oxygen atoms per two cobalt atoms, corresponding to the high-oxidized state (Figure 1c,d). Figure 1 shows the most stable configurations for which we have studied the magneto-optical properties.

The ferromagnetic (FM) and antiferromagnetic (AFM) spin configurations of oxide Co NWs have been considered the most preferable magnetic structures for pure Co nanowires on vicinal Pt surfaces [6,10,31,32]. The occurrence of these two magnetic configurations has also been observed experimentally for cobalt oxide thin films, as reported recently by Helen et al. [46]. In Table 1 the values of exchange parameter $J^{1,2}_{Co-Co}$, directly related to the energy difference between ferromagnetic and antiferromagnetic spin configurations ($\Delta E = E_{FM} - E_{AFM}$), for oxide Co NWs are presented. To describe the effect of oxidation on the magnetic properties of supported Co nanowires the magnetic properties of pure Co NWs have been considered. We found that the ground state of pure Co NW is ferromagnetic with local magnetic moment of Co atoms about 2 μ_B for both vicinal Pt surfaces (Pt(322) and Pt(332)), while AFM spin configuration has shown the decreasing of local magnetic moment of Co atoms up to 1.8 μ_B. Based on previous studies, the FM and AFM spin magnetic states are maintained through direct and indirect exchange interaction between Co atoms in oxide nanowires (see Figure 1). The indirect exchange J^{1}_{Co-Co} between Co atoms is realized through O atom due to the formation of complex hybridized energy bands between the *p*-states of oxygen atoms and *d*-states of cobalt atoms in the nanowire. The direct exchange J^{2}_{Co-Co} between Co atoms is realized due to the formation of the hybridized band between *d*-states of neighboring Co atoms in the nanowires (Figure 1e).

Table 1. Magnetic moment (μ_{Co}) and exchange parameter (J_{Co-Co}) through oxygen atoms, direct exchange channels [31,32].

	CoO NW		**CoO_2 NW**	
	Pt(332)	**Pt(322)**	**Pt(332)**	**Pt(322)**
Ground state	FM	AFM	FM	AFM
μ_{Co}	1.5 μ_B	+/−1.5 μ_B	0.6 μ_B	+/−0.2 μ_B
J_{Co-Co}	−5 meV	15 meV	−8 meV	7 meV

The energy difference ΔE corresponding to J_{Co-Co} = 31 meV for pure Co NW demonstrates the relatively higher stability of the ferromagnetic state with respect to the antiferromagnetic one, that makes the magnetic transition between these two states to be a rather energetically unfavorable process for Co spins. The oxidation of pure Co NW leads to the suppression of its magnetic behavior on both vicinal Pt surfaces. The herewith ground state of CoO and CoO_2 nanowires on the Pt(332) surface remains ferromagnetic, with local magnetic moments of Co atoms about 1.5 μ_B and 0.6 μ_B, respectively, while the ground states of these oxides on Pt(322) surface are antiferromagnetic with the values of local magnetic moments about 1.5 μ_B and 0.2 μ_B. Besides that, our calculations demonstrate the significant decrease in the energy differences ΔE for these oxides in comparison to pure Co nanowires (see Table 1). Moreover, our calculations have shown the dependence of the energy difference ΔE on the degree of oxidation and the local atomic structure of the step edge. We have found that ΔE in a high oxidized state is smaller than in a low oxidized state. Besides that, ΔE for CoO NW in a low oxidized state on Pt(332) surface is two times

less than on Pt(322) one. Here, it is worth noting that the smaller value of ΔE makes the magnetic structure to be more attractive for the manipulation of its magnetic states by means of ultrafast EM laser pulses in the optical, UV, infrared or THz ranges [3]. Based on the fact that we have considered CoO NW as a good candidate for such laser applications and its optical characteristics have to be estimated. For this purpose, we have calculated the effective optical constants, such as refractive index n and extinction coefficient κ as a function of frequency and magnetic state (FM and AFM) of Co NW on both Pt(332) and Pt(322) surfaces. At first, the frequency dependence of n was calculated and the obtained results are shown in Figure 2.

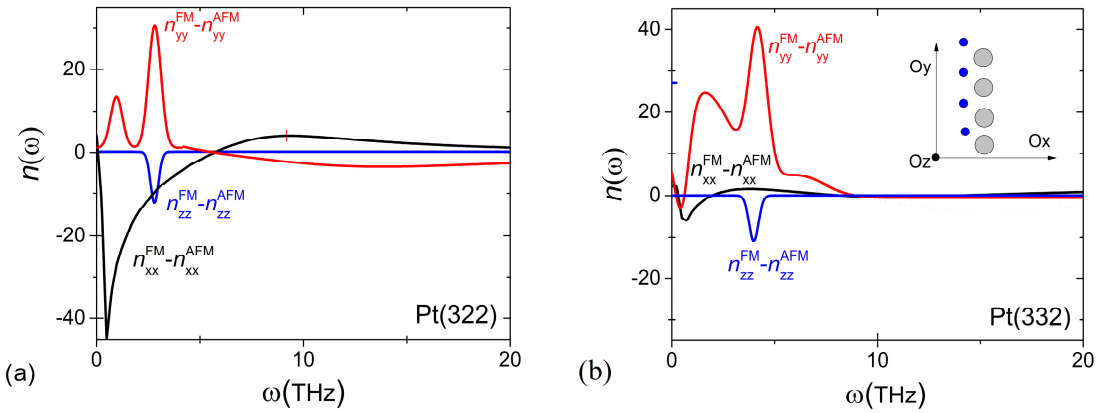

Figure 2. Refractive indexes differences of CoO nanowire on Pt(322) (**a**) and Pt(332) (**b**) surfaces in low oxidized state for FM and AFM magnetic configurations.

In Figure 2, one can see all components of the refractive index (n_{xx}, n_{yy} and n_{zz}). The n_{xx} and n_{yy} components of the refractive index represent in-plain components of n; moreover, the n_{yy} component is aligned with the direction of NW growth. The n_{zz} component is co-directed with the normal to the Pt surface and coincides with the direction of the EM wave propagation in our model. We constructed the spectral difference of the refractive indexes between AFM and FM configurations of CoO NW for each component of the refractive index (n_{xx} and n_{yy}, n_{zz}). We found the emergence of two resonant peaks in difference spectra for Δn_{xx} component in the terahertz range with frequencies 1.5 THz and 3 THz. The positions of peaks are the same for both types of platinum surfaces. For the Δn_{yy} component, only one low-frequency peak at 1.5 THz was found. In addition, a high-frequency peak at 3 THz was detected in refractivity spectra for the n_{zz} component. As a result, the study of the refractivity of CoO NW revealed a change in the optical response of oxide Co NW for different magnetic configurations. These calculations demonstrate that EM radiation in the THz range can be considered a proper means for detecting the magnetic state of oxide Co nanowires [3,5].

We also studied the frequency dependence of extinction coefficient κ on magnetic coupling within a wire. For this purpose, the frequency dependence of the extinction coefficient for FM and AFM CoO NW was calculated (Figure 3). Figure 3 presents the frequency dependence of the extinction coefficient κ on Pt(322) surface, while the same dependence has been obtained for Pt(332) surface. Our calculations revealed the strong dependence of the extinction coefficient on the magnetic coupling into a wire. The most significant changes were found in the low-frequency (THz) region of spectra. We found the anisotropy of the extinction coefficient of AFM CoO NWs in the terahertz range. The first-principles calculations have shown the strong absorption of the y-component in comparison to the x-component of the EM radiation in the terahertz range. Furthermore, we found the isotropic absorption of EM waves in the ferromagnetic configuration of CoO NW.

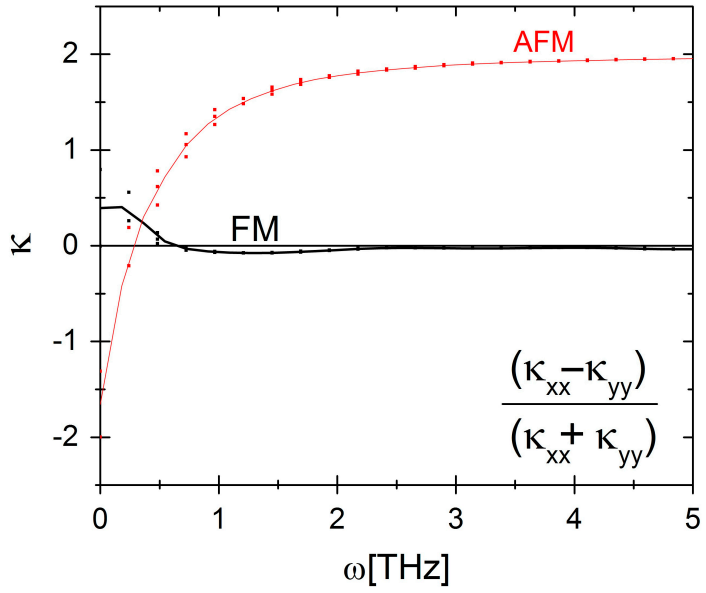

Figure 3. Extinction coefficient of CoO nanowire on Pt(322) in low oxidized state for FM and AFM spin configurations.

Finally, we demonstrate our calculations of surface dielectric anisotropy (SDA) for CoO NW on Pt(322) surface in both FM and AFM spin configurations and in the same frequency range [47]. The study of SDA spectra makes it possible to analyze the relationship between the polarization of the transmitted or reflected light and the magnetic coupling in the nanowire. To highlight the effect of the optical response from supported magnetic oxide Co nanowires, we also constructed SDA spectra of the flat and vicinal platinum surfaces, as well as a platinum bulk. At first, we studied the SDA spectra of the flat Pt(111) surface in order to determine the specific response of the system associated with the formation of inhomogeneities of the substrate (step edges, atomic magnetic wires or one-dimensional metal oxides). To analyze the effect of surface inhomogeneities on the SDA spectra we have built up a model structure of Pt(111) surface with a cut-out stripe with {100}- and {111}-type facets, which simulated two types of step edges, that coincide in atomic structure with the steps of Pt(322) and Pt(332) vicinal surfaces, respectively. This analysis made it possible to select the operating range of the spectrum for our study that is most sensitive to the surface structure, f.e. step edges or surface-supported oxide Co nanowires. The SDA spectra of Pt(111) surface with a cut-out stripe contains two distinct peaks: a low-energy peak located in the spectral range (0–1 eV) and a high-energy peak at (5–7 eV). The low-energy peak (0–1 eV) has the same structure and position for both the flat surface and the surface with the cut-out stripe, as well as for the Pt bulk. Only the position of the high-energy (5–7 eV) peak is sensitive to the surface structure and surface inhomogeneities. The comparison of the SDA spectra for a flat Pt (111) surface with a cut-out strip and for Pt(322) and Pt(332) vicinal surfaces showed that only the high-energy peak corresponds to the response of the step edges. The flat surface does not have such a feature in this spectral range, the similar result was obtained earlier in a theoretical work [43]. The study of the SDA spectra for CoO nanowires on Pt(322) surface also revealed the emergence of a singular peak in the SDA at a frequency value corresponding to ~6 eV (Figure 4). Our study has shown that a change of magnetic coupling between Co atoms into a nanowire leads to a slight shift of this peak position to the high-frequency range in ferromagnetic CoO NWs compared to antiferromagnetic ones.

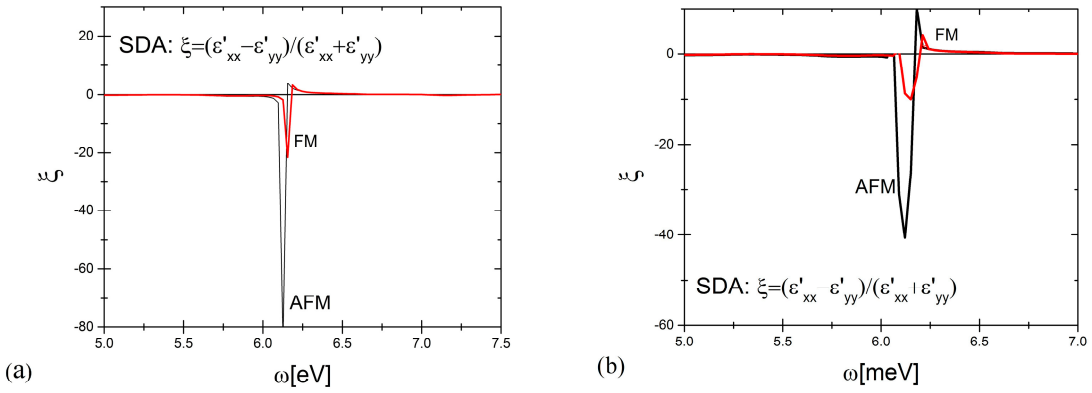

Figure 4. SDA spectra of CoO nanowires on Pt(322) in AFM (black curve)) and FM (red curve) spin configurations for high-energy (**a**) and for low-energy ranges (**b**).

Despite the fact that the low-energy peak (0–1 eV) is insensitive to the surface structure and is not typical for the study of the surface inhomogeneities and surface-supported nanostructures, f.e. nanowires, this peak can be sensitive to the magnetic spin state of the oxide Co nanowires studied in this work. Therefore, we have investigated the effect of magnetic coupling in the wire on the position of the peak in the low-energy range. The study of the SDA spectra revealed the emergence of a singular peak in the SDA at frequency ~1.5 THz (6 meV), corresponding to a low-frequency resonant peak in refractivity spectra (see Figure 4b). However, we did not find a resonant peak in SDA corresponding to a high-frequency peak in the refractivity spectra at 3 THz, which proves the influence of magnetic coupling between Co spins in the nanowire on the polarization of transmitted light only at frequency ~1.5 THz. We found a shift of the 1.5 THz peak to the high-frequency range in ferromagnetic CoO NWs compared to antiferromagnetic counterparts of the ~6 eV high-energy peak mentioned above.

The band structure calculations of CoO NW have shown that the obtained difference in its optical characteristic is caused by the changes in its electronic structure in different magnetic states. The formation of the complex hybrid band between the *d*-subband of Co atoms and *p*-subbands of O atom was established in the band structure of CoO NW, which occurred due to strong Co-O interaction [31,32]. The structure of this hybrid band is different for FM and AFM spin configurations. Furthermore, the band structure analysis revealed that singular peak at frequency ~6 eV for FM and AFM spin configurations of CoO NW on Pt(322) surface occurs due to the change of spatial orientations of subbands responsible for the re-reflection of the light in these two different magnetic configurations.

4. Conclusions

In conclusion, the results of first-principles calculations revealed the effect of magnetic coupling between cobalt atoms on the refractivity and extinction spectra of 1D Co oxides governed by Co-O interactions within nanowires at the step edge. The emergence of a sharp pronounced peak in the spectral difference of the refractive indexes has been observed between ferromagnetic and antiferromagnetic spin configurations of the nanowire. We found an anisotropy of extinction coefficient of oxide Co nanowires in the antiferromagnetic spin configuration in the terahertz range in contrast to the ferromagnetic one. The study of SDA spectra for CoO nanowires on Pt(322) surface also revealed the emergence of a singular peak in SDA at frequency of ~1.5 THz. The study of SDA spectra makes it possible to analyze the relationship between the polarization of the transmitted and reflected light and the magnetic coupling in the wire. Our study has shown that a change in the magnetic coupling in the wire leads to a slight shift of this peak position to the high-frequency range in ferromagnetic CoO NWs compared to antiferromagnetic ones.

Author Contributions: Conceptualization, D.I.B. and K.M.T.; methodology D.I.B.; software, D.I.B. and K.M.T.; validation, K.M.T. and E.M.S.; resources, D.I.B. and K.M.T.; data curation, K.M.T.; writing—original draft preparation, K.M.T. and E.M.S.; writing—review and editing, K.M.T., E.M.S. and D.I.B.; visualization, E.M.S.; project administration, D.I.B. All authors have read and agreed to the published version of the manuscript.

Funding: This research received no external funding.

Data Availability Statement: Not applicable.

Acknowledgments: This work has been carried out using the facilities of the Joint Supercomputer Center of the Russian Academy of Sciences (JSCC RAS) and computational resources of MCC NRC «Kurchatov Institute».

Conflicts of Interest: The authors declare no conflict of interest.

References

1. Belotelov, V.I.; Akimov, I.A.; Pohl, M.; Kotov, V.A.; Kasture, S.; Vengurlekar, A.S.; Bayer, M. Enhanced magneto-optical effects in magnetoplasmonic crystals. *Nat. Nanotechnol.* **2011**, *6*, 370–376. [CrossRef]
2. Kimel, A.V.; Kirilyuk, A.; Usachev, P.A.; Pisarev, R.V.; Balbashov, A.M.; Rasing, T. Ultrafast non-thermal control of magnetization by instantaneous photomagnetic pulses. *Nature* **2005**, *435*, 655–657. [CrossRef]
3. Bigot, J.-Y.; Vomir, M.; Beaurepaire, E. Coherent Ultrafast magnetism induced by femtosecond laser pulses. *Nat. Phys.* **2009**, *5*, 515–520. [CrossRef]
4. Berritta, M.; Mondal, R.; Carva, K.; Oppeneer, P.M. Ab initio theory of coherent laser-induced magnetization in metals. *Phys. Rev. Lett.* **2016**, *117*, 137203. [CrossRef]
5. López-Ortega, A.; Zapata-Herrera, M.; Maccaferri, N.; Pancaldi, M.; Garcia, M.; Chuvilin, A.; Vavassori, P. Enhanced magnetic modulation of light polarization exploiting hybridization with multipolar dark plasmons in magnetoplasmonic nanocavities. *Light Sci. Appl.* **2020**, *9*, 49. [CrossRef]
6. Gambardella, P.; Dallmeyer, K.A.; Maiti, M.C.; Malagoli, W.; Eberhardt, K.; Kern, C. Carbone Ferromagnetism in one-dimensional monatomic metal chains. *Nature* **2002**, *416*, 301–304. [CrossRef]
7. Gambardella, P.; Dallmeyer, A.; Maiti, K.; Malagoli, M.C.; Rusponi, S.; Ohresser, P.; Eberhardt, W.; Carbone, C.; Kern, K. Oscillatory magnetic anisotropy in one-dimensional atomic wires. *Phys. Rev. Lett.* **2004**, *93*, 077203. [CrossRef]
8. Cheng, R.; Guslienko, K.Y.; Fradin, F.Y.; Pearson, J.E.; Ding, H.F.; Li, D.; Bader, S.D. Step-decorated ferromagnetic Fe nanostripes on Pt(997). *Phys. Rev. B* **2005**, *72*, 014409. [CrossRef]
9. Cheng, R.; Ayieta, E.; Losovyj, Y.B. Electronic states of Fe nanostructures on Pt(997) surface. *J. Vac. Sci. Technol. A* **2008**, *26*, 673–677. [CrossRef]
10. Baud, S.; Ramseyer, C.; Bihlmayer, G.; Blügel, S. Relaxation effects on the magnetism of decorated step edges: Co/Pt(664). *Phys. Rev. B* **2006**, *73*, 104427. [CrossRef]
11. Bazhanov, D.I.; Hergert, W.; Stepanyuk, V.S.; Katsnelson, A.A.; Rennert, P.; Kokko, K.; Demangeat, C. One-dimensional magnetism of Rh chains on the Ag(001) surface. *Phys. Rev.B* **2000**, *62*, 6415–6420. [CrossRef]
12. Bellini, V.; Papanikolaou, N.; Zeller, R.; Dederichs, P.H. Magnetic 4d monoatomic rows on Ag vicinal surfaces. *Phys. Rev. B* **2001**, *64*, 094403. [CrossRef]
13. Tsysar, K.M.; Smelova, E.M.; Bazhanov, D.I.; Saletsky, A.M. Effect of stretching-contraction deformations on the magnetic ordering state of mixed Pd-Fe nanowires. *JETP Lett.* **2011**, *94*, 246–251. [CrossRef]
14. Tsysar, K.M.; Bazhanov, D.I.; Smelova, E.M.; Saletsky, A.M. Emergence of giant magnetic anisotropy in freestanding Au/Co nanowires. *Appl. Phys. Lett.* **2012**, *101*, 043108. [CrossRef]
15. Tsysar, K.M.; Kolesnikov, S.V.; Saletsky, A.M. Magnetization dynamics of mixed Co-Au chains on Cu(110) substrate: Combined ab initio and kinetic Monte Carlo study. *Chin. Phys. B* **2015**, *24*, 097302. [CrossRef]
16. Hammer, L.; Meier, W.; Klein, A.; Landfried, P.; Schmidt, A.; Heinz, K. Hydrogen-induced self-organized nanostructuring of the Ir(100) surface. *Phys. Rev. Lett.* **2003**, *91*, 156101. [CrossRef]
17. Alnot, M.; Fusy, J. Study of Cobalt films deposited on Pt(110)(1×2). *Appl. Surf. Sci.* **1992**, *55*, 209–219. Available online: http://www.sciencedirect.com/science/article/pii/016943329290112B (accessed on 23 September 2002). [CrossRef]
18. Moulas, G.; Lehnert, A.; Rusponi, S.; Zabloudil, J.; Etz, C.; Ouazi, S.; Etzkorn, M.; Bencok, P.; Gambardella, P.; Weinberger, P.; et al. High magnetic moments and anisotropies for $Fe_x Co_{1-x}$ monolayers on Pt(111). *Phys. Rev. B* **2008**, *78*, 214424. [CrossRef]
19. Vukajlovič, F.R.; Popovič, Z.S.; Baldereschi, A.; Šljivančanin, Ž. Effect of adsorbed H atoms on magnetism in monoatomic Fe wires at Ir(100). *Phys. Rev. B* **2010**, *81*, 085425. [CrossRef]
20. Urdaniz, M.C.; Barral, M.A.; Llois, A.M.; Sa'ul, A. Magnetic interactions in 3d metal chains on $Cu_2X/Cu(001)$ (x = N; O): Comparison with corresponding unsupported chains. *Phys. Rev. B* **2014**, 195423. [CrossRef]
21. Korobova, J.G.; Nikitina, I.A.; Bazhanov, D.I.; Ruiz-Díaz, P. Oxygen-Mediated Superexchange Interactions and Their Impact on the Structural Stability, Magnetic Order, and Magnetocrystalline Anisotropy of One-Dimensional Co-Oxide Chains on Rh(553) Step-Surfaces. *J. Phys. Chem. C* **2020**, *124*, 26026–26036. [CrossRef]

22. Koshelev, Y.S.; Bazhanov, D.I. Effect of Oxygen on the quantum, magnetic, and thermodynamic properties of Co nanowires on the reconstructed anisotropic (1 × 2)/Au(110) and (1 × 2)/Pt(110) surfaces: Ab initio approach. *J. Exp. Theor. Phys.* **2018**, *127*, 179–188. [CrossRef]
23. Maca, F.C.V.; Kudrnovský, J.; Drchal, V.; Redinger, J. Influence of Oxygen and Hydrogen adsorption on the magnetic structure of an ultrathin Iron film on an Ir(001) surface. *Phys. Rev. B* **2013**, *201388*, 045423. [CrossRef]
24. Ma, X.-D.; Nakagawa, T.; Yokoyama, T. Effect of surface chemisorption on the spin reorientation transition in magnetic ultrathin Fe film on Ag(001). *Surf. Sci.* **2006**, *600*, 4605–4612. Available online: http://www.sciencedirect.com/science/article/pii/S003960280600817X (accessed on 14 August 2006). [CrossRef]
25. Jacobson, P.; Muenks, M.; Laskin, G.; Brovko, O.; Stepanyuk, V.; Ternes, M.; Kern, K. Potential energy-driven spin manipulation via a controllable Hydrogen ligand. *Sci. Adv.* **2017**, *3*, e1602060. Available online: https://advances.sciencemag.org/content/3/4/e1602060.full.pdf (accessed on 17 April 2017). [CrossRef]
26. Netzer, F.P. "Small and beautiful"—The novel structures and phases of nano-oxides. *Surf. Sci.* **2010**, *604*, 485–489. Available online: http://www.sciencedirect.com/science/article/pii/S003960281000004X (accessed on 11 January 2010). [CrossRef]
27. Li, F.; Allegretti, F.; Surnev, S.; Netzer, F.P. Atomic engineering of oxide nanostructure superlattices. *Surf. Sci.* **2010**, *604*, L43–L47. Available online: http://www.sciencedirect.com/science/article/pii/S0039602810002190 (accessed on 24 May 2010). [CrossRef]
28. Ma, L.Y.; Picone, A.; Wagner, M.; Surnev, S.; Barcaro, G.; Fortunelli, A.; Netzer, F.P. Structure and electronic properties of CoO nanostructures on a vicinal Pd(100) surface. *J. Phys. Chem. C* **2013**, *117*, 18464–18474. [CrossRef]
29. Surnev, S.; Allegretti, F.; Parteder, G.; Franz, T.; Mittendorfer, F.; Andersen, J.N.; Netzer, F.P. One-dimensional oxide-metal hybrid structures: Site-specific enhanced reactivity for CO oxidation. *ChemPhysChem* **2010**, *11*, 2506–2509. [CrossRef]
30. Schoiswohl, J.; Mittendorfer, J.F.; Surnev, S.; Ramsey, M.G.; Andersen, J.N.; Netzer, F.P. Chemical reactivity of Ni-Rh nanowires. *Phys. Rev. Lett.* **2006**, *97*, 126102. [CrossRef]
31. Tsysar, K.M.; Koshelev, Y.; Bazhanov, D.I.; Smelova, E.M. Emergence of magnetic transition in Cobalt oxide nanowires on vicinal Pt substrate. *IEEE Magn. Lett.* **2021**, *13*, 1–5. [CrossRef]
32. Tsysar, K.M.; Smelova, E.M.; Bazhanov, D.I. Magneto-Optical Properties of Oxidized Co Nanowires on Pt Substrate. *Phys. Status Solidi B* **2022**, *259*, 2200018. [CrossRef]
33. Von Kugelgen, S.; Krzyaniak, M.D.; Gu, M.; Puggioni, D.; Rondinelli, J.M.; Wasielewski, M.R.; Freedman, D.E. Spectral Addressability in a Modular Two Qubit System. *J. Am. Chem. Soc.* **2021**, *143*, 8069–8077. [CrossRef]
34. Bandlow, J.; Kaghazchi, P.; Jacob, T.; Papp, C.; Tränkenschuh, B.; Streber, R.; Lorenz, M.P.A.; Fuhrmann, T.; Denecke, R.; Steinrück, H.-P. Oxidation of stepped Pt(111) studied by X-ray photoelectron spectroscopy and density functional theory. *Phys. Rev. B* **2011**, *83*, 174107. [CrossRef]
35. Kresse, G.; Furthmuller, J. Efficient iterative schemes for ab initio total-energy calculations using a plane-wave basis Se. *Phys. Rev. B* **1996**, *54*, 11169. [CrossRef]
36. Kohn, W.; Sham, L.J. Self–consistent equations including exchange and correlation effects. *Phys. Rev. A* **1965**, *140*, 1133–1138. [CrossRef]
37. Shishkin, M.; Kresse, G. Implementation and performance of the frequency-dependent GW method within the PAW framework. *Phys. Rev. B* **2006**, *74*, 035101. [CrossRef]
38. Blochl, P.P. Projector augmented-wave method. *Phys. Rev. B* **1994**, *50*, 17953. [CrossRef]
39. Monkhorst, H.J.; Pack, J.D. Special points for Brillouin-zone integrations. *Phys. Rev. B* **1976**, *13*, 5188. [CrossRef]
40. Klikovits, J.; Schmid, M.; Merte, L.R.; Varga, P. Step-Orientation-Dependent Oxidation: From 1D to 2D Oxides. *Phys. Rev. Lett.* **2008**, *101*, 266104. [CrossRef]
41. Dudarev, S.L.; Botton, G.A.; Savrasov, S.Y.; Humphreys, C.J.; Sutton, A.P. Electron-energy-loss spectra and the structural stability of nickel oxide: An lsda+u study. *Phys. Rev. B* **1998**, *57*, 1505–1509. [CrossRef]
42. Wang, L.; Maxisch, T.; Ceder, G. Oxidation energies of transition metal oxides within the GGA+U framework. *Phys. Rev. B* **2006**, *73*, 195107. [CrossRef]
43. Mittendorfer, F.; Weinert, M.; Podloucky, R.; Redinger, J. Strain and structure driven complex magnetic ordering of a coo overlayer on ir(100). *Phys. Rev. Lett.* **2012**, *109*, 015501. [CrossRef]
44. Gajdoš, M.; Hummer, K.; Kresse, G.; Furthmüller, J.; Bechstedt, F. Linear optical properties in the projector-augmented wave methodology. *Phys. Rev. B* **2006**, *73*, 045112. [CrossRef]
45. Shishkin, M.; Marsman, M.; Kresse, G. Accurate Quasiparticle Spectra from Self-Consistent GW Calculations with Vertex Corrections. *Phys. Rev. Lett.* **2007**, *99*, 246403. [CrossRef]
46. Helen, V.; Joseph Prince, J. Influence of annealing on the structural, optical and magnetic properties of CoO thin films. *Mater. Res. Innov.* **2019**, *23*, 200–206. [CrossRef]
47. Harl, J.; Kresse, G.; Sun, L.D.; Hohage, M.; Zeppenfeld, P. Ab initio reflectance difference spectra of the bare and adsorbate covered Cu(110) surfaces. *Phys. Rev. B* **2007**, *76*, 035436. [CrossRef]